

Metformin Augments Panobinostat's Anti-Bladder Cancer Activity by Activating AMP-Activated Protein Kinase^{1,2}



Kazuki Okubo, Makoto Isono, Takako Asano and Akinori Sato

Department of Urology, National Defense Medical College, 3-2 Namiki, Tokorozawa, Saitama 359-8513, Japan

Abstract

Panobinostat, a histone deacetylase inhibitor, induces histone acetylation and acts against cancer but attenuates its anticancer activity by activating the mammalian target of rapamycin (mTOR) pathway. AMP-activated protein kinase (AMPK) is a cellular energy sensor that reportedly inhibits the mTOR pathway. The antidiabetic drug metformin is also a potent AMPK activator and we investigated whether it augmented panobinostat's antineoplastic activity in bladder cancer cells (UMUC3, J82, T24 and MBT-2). Metformin enhanced panobinostat-induced apoptosis and the combination inhibited the growth of bladder cancer cells cooperatively *in vitro* and *in vivo*. As expected, metformin increased the phosphorylation of AMPK and decreased the panobinostat-caused phosphorylation of S6 ribosomal protein, thus inhibiting the panobinostat-activated mTOR pathway. The AMPK activation was shown to play a pivotal role in the combination's action because the AMPK inhibitor compound C attenuated the combination's anticancer activity. Furthermore, the AMPK activation by metformin enhanced panobinostat-induced histone and non-histone acetylation. This acetylation was especially remarkable in the proteins in the detergent-insoluble fraction, which would be expected if the combination also induced endoplasmic reticulum stress.

Translational Oncology (2019) 12, 669–682

Introduction

Bladder cancer is the second most common malignancy of the genitourinary tract and is associated with significant morbidity and mortality [1]. So far there is no curative treatment for patients with advanced bladder cancer. Cisplatin-based combinations such as gemcitabine and cisplatin or methotrexate, vinblastine, doxorubicin and cisplatin are the standard regimens used for treating patients with metastatic bladder cancer but do not significantly prolong overall survival or progression-free survival [2,3]. Immunotherapeutic agents targeting the programmed cell death protein 1 or programmed death-ligand have attracted enormous attention but have only prolonged overall survival by several months [4–6]. Clearly there is urgent need for novel treatment strategies against advanced bladder cancer.

Histone acetylation is an emerging strategy for treating cancer [7]. Histone deacetylase (HDAC) inhibitors are a new class of anticancer agents targeting the enzymes that remove acetyl groups from lysine residues in histones [8]. Panobinostat is an HDAC inhibitor approved by the Food and Drug Administration for the treatment of multiple myeloma [9,10], but has limited efficacy against solid tumors [11,12]. One possible reason for this limited effectiveness might be panobinostat's activation of the mammalian target of rapamycin

(mTOR) pathway [13]. Inhibiting the panobinostat-activated mTOR pathway is therefore thought to be a rational approach to enhancing panobinostat's anticancer activity.

AMP-activated protein kinase (AMPK) is a cellular energy sensor activated by ATP depletion [14]. Since AMPK can inhibit the mTOR pathway, activating AMPK is considered to be a novel strategy for killing cancer cells [14–17]. We thought that combining panobinostat with an AMPK-activating agent would enhance panobinostat's anticancer activity because it would inhibit panobinostat-induced mTOR activation.

In the present study we investigated the combined effect of panobinostat and metformin on bladder cancer cells both *in vitro* and

Address all correspondence to: Akinori Sato, Department of Urology, National Defense Medical College, 3-2 Namiki, Tokorozawa, Saitama 359-8513, Japan.

¹ Funding sources: This work was supported by JSPS KAKENHI [Grant Number JP18K09183]. ² Conflict of interest: None reported. Received 7 February 2019; Accepted 11 February 2019

© 2019 The Authors. Published by Elsevier Inc. on behalf of Neoplasia Press, Inc. This is an open access article under the CC BY-NC-ND license (<http://creativecommons.org/licenses/by-nc-nd/4.0/>).

1936-5233/19

<https://doi.org/10.1016/j.tranon.2019.02.001>

in vivo. Metformin is a commonly used antidiabetic drug shown to activate AMPK [18–20], so we thought it would enhance panobinostat's anticancer activity. We also expected the combination to induce histone acetylation cooperatively because metformin-activated AMPK would induce histone acetylation by inhibiting acetyl CoA carboxylase (ACC) [20–22].

Materials and Methods

Cell Cultures

Human bladder cancer cells (UMUC3, J82 and T24) were purchased from the American Type Culture Collection (Rockville, MD, USA) and murine bladder cancer cells (MBT-2) were purchased from Japanese Collection of Research Bioresources Cell Bank (Osaka, Japan). The cells were cultured in the recommended media (Roswell Park Memorial Institute medium, Minimum Essential medium and McCoy's 5A medium) supplemented with 10% fetal bovine serum and 1.0% penicillin/streptomycin (Invitrogen, Carlsbad, CA, USA) at 37 °C under 5% CO₂ in a humidified incubator.

Reagents

Panobinostat purchased from LC Laboratories (Boston, MA, USA), suberoylanilide hydroxamic acid (SAHA) purchased from Cayman Chemical (Ann Arbor, MI, USA), entinostat purchased from

Table 1. Mean inhibitory concentrations (IC₅₀) of panobinostat in bladder cancer cells.

	Panobinostat (nM)
UMUC3	166.7
J82	242.2
T24	71.2
MBT-2	192

Selleck Chemicals (Houston, TX, USA), and 5-aminoimidazole-4-carboxamide (AICAR) purchased from Sigma-Aldrich (St Louis, MO, USA) were dissolved in dimethyl sulfoxide. Metformin purchased from Enzo Life Sciences (Farmingdale, NY, USA) and compound C purchased from Selleck Chemicals were dissolved in distilled water. These agents were stored in the dark at –80 °C or –20 °C until use.

Cell Viability Assay

Cell viability was assessed by MTS assay using a CellTiter 96 Aqueous kit (Promega, Madison, WI, USA) according to the manufacturer's protocol. 5×10^3 cells were plated in a 96-well culture plate 1 day before drug treatment. After 48-hour treatment with varying doses of single drug or combined therapy, the medium was replaced with 20 μ L MTS solution buffer in 100 μ L fresh medium and the plates were incubated for another hour. The plates were then read at a wavelength of 490 nm in a microplate autoreader.

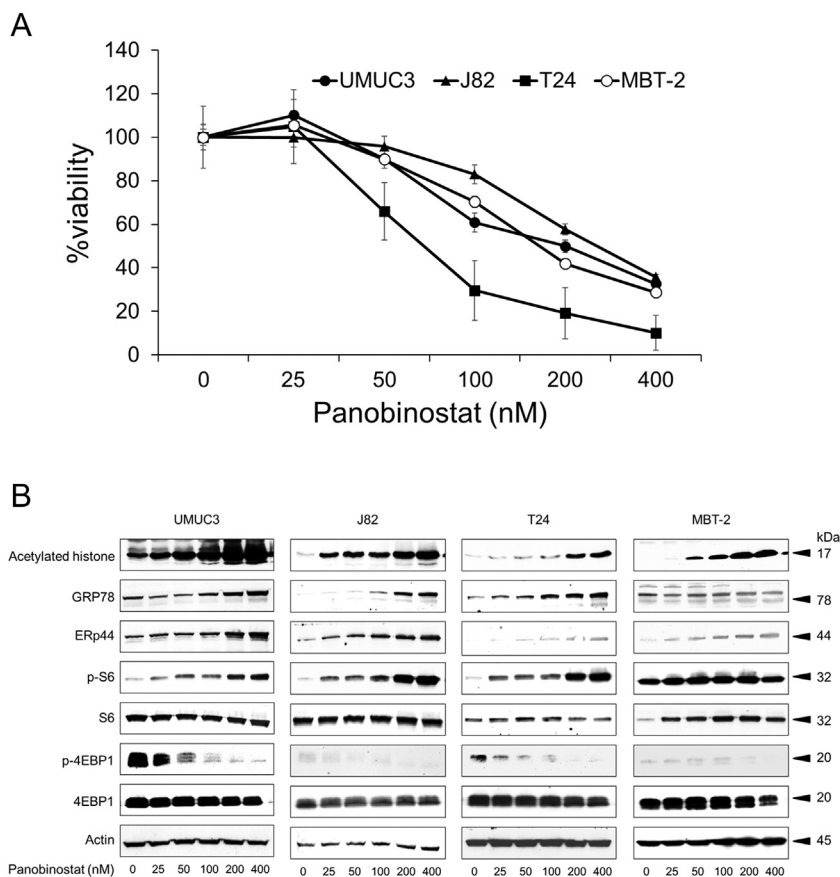


Figure 1. Panobinostat induced histone acetylation and endoplasmic reticulum (ER) stress but also activated the mammalian target of rapamycin pathway. (A) MTS assay. Cells were treated for 48 hours with 25–400 nM panobinostat, and cell viability was measured using MTS assay. Bars represent mean \pm SD, $n = 12$. (B) Western blotting for acetylated histone, the ER stress markers glucose-regulated protein (GRP) 78 and endoplasmic reticulum resident protein 44 (ERp44), S6 ribosomal protein (S6), and eukaryotic translation initiation factor 4E-binding protein 1 (4EBP1). Cells were treated for 48 hours with 25–400 nM panobinostat. Actin was used for the loading control. Representative blots are shown.

and the results expressed as the mean optical density of the six-well set for each group.

Colony Formation Assay

One hundred fifty individual cells were seeded into 6-well plates 1 day before being treated with 100 nM panobinostat and/or 20 mM metformin. After 48-hour treatment, the cells were given fresh media and cultured for 1–2 weeks. The colonies were

fixed with 100% methanol, stained with Giemsa's solution and counted.

Allograft Experiment

The experimental protocol for this *in vivo* experiment was approved by the institutional Animal Care and Use Committee of National Defense Medical College. 1×10^7 MBT-2 cells were implanted subcutaneously into the posterior flank region of C3H/He

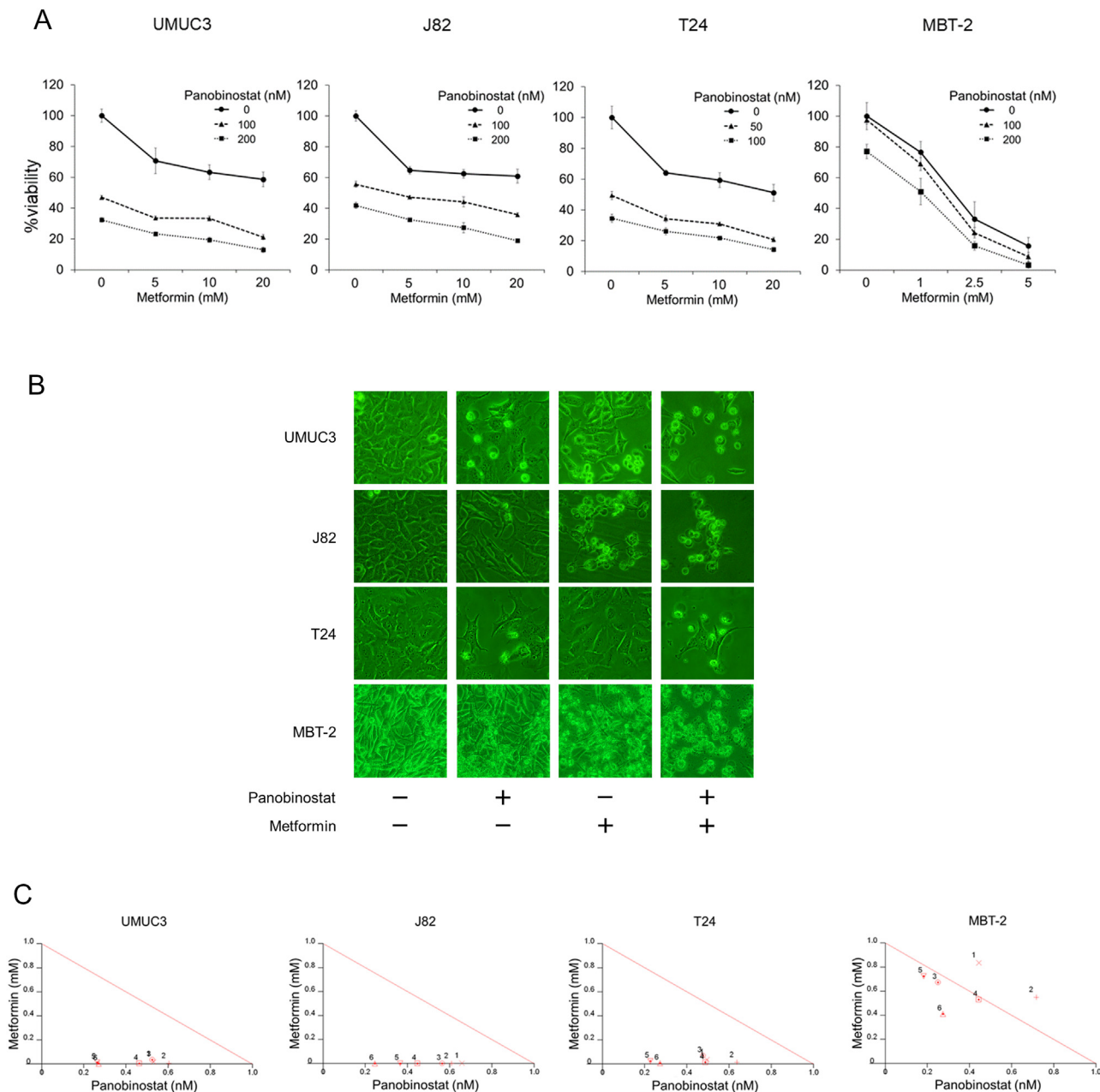


Figure 2. The combination of panobinostat and metformin inhibited bladder cancer growth *in vitro* effectively. (A) MTS assay. Cells were treated for 48 hours with 50–200 nM panobinostat and/or 1–20 mM metformin, and cell viability was measured using MTS assay. Bars represent mean \pm SD, n = 6. (B) Photomicrographs after 48-hour treatment. Note that cells treated by the combination had a round and swollen morphology and most of them were floating as compared with untreated cells. Original magnification, 200 \times . (C) Isobologram analysis for the combination of panobinostat and metformin. (D) MTS assay. Cells were treated for 48 hours with 5–10 μ M suberoylanilide hydroxamic acid (SAHA) or entinostat and/or 5–20 mM metformin, and cell viability was measured using MTS assay. Bars represent mean \pm SD, n = 6. (E) Isobologram analysis for the combination of SAHA or entinostat and metformin. (F) Colony formation assay. 150 cells were treated for 48 hours with 100 nM panobinostat and/or 20 mM metformin. The cells were then given fresh media and allowed to grow for 2 weeks. Bar graphs show the number of colonies expressed as percentage of control. Mean \pm SD, n = 3. C, control; P, 100 nM panobinostat; M, 20 mM metformin. *P = .0495.

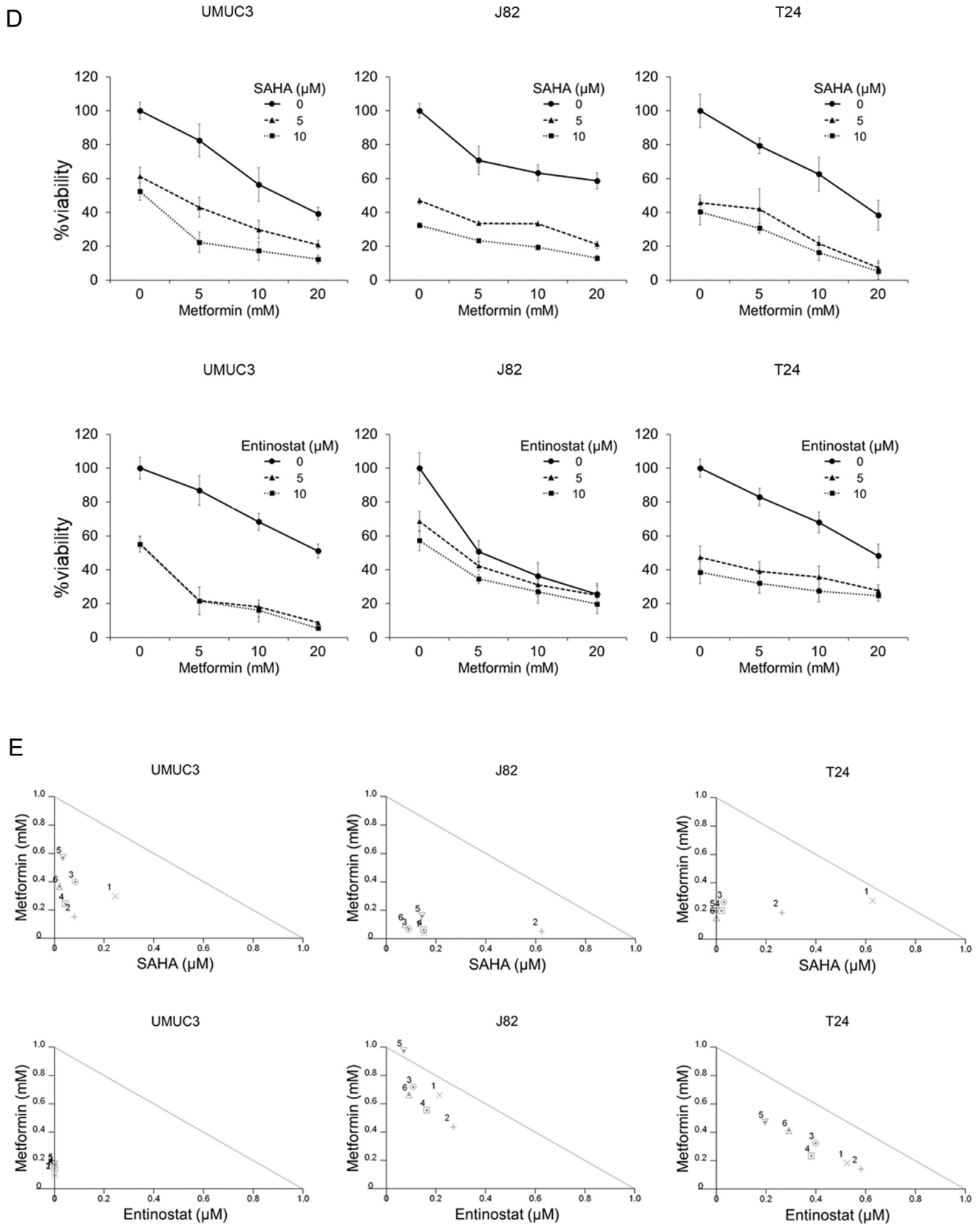


Figure 2 (continued)

mice purchased from CLEA Japan (Tokyo, Japan) and treatment was initiated 7 days later (day 1), when all the mice exhibited measurable tumors. The mice were randomly divided into control and three

treatment groups ($n = 5$ each). The treated mice received intraperitoneal injections of either panobinostat (2 mg/kg) or metformin (100 mg/kg) or both, while the control mice received vehicle only. The

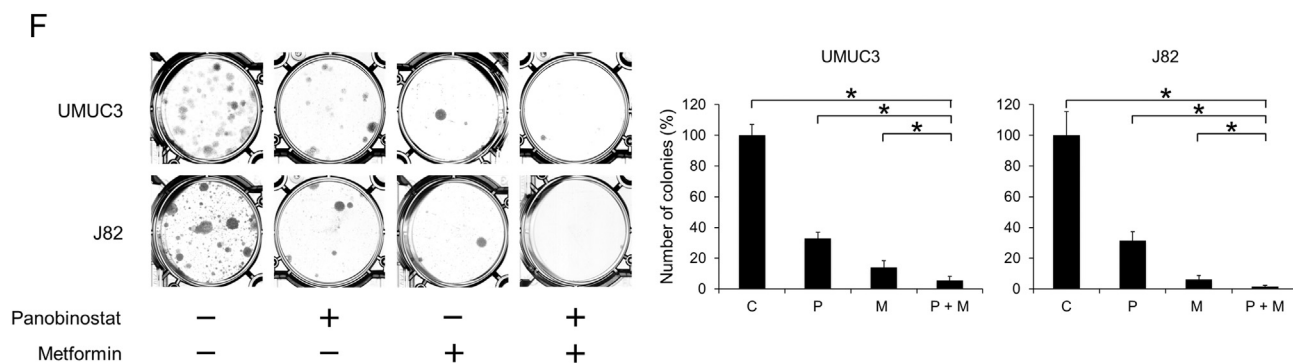


Figure 2. (continued)

injections were given once a day for 20 days (10 days on, 2 days off and 10 days on). Tumor volume and body weights were measured every 4 or 5 days. Tumor volumes were estimated using the following formula: volume = 0.5 × length × width². The mice were sacrificed when their tumor volume increased above 3000 mm³, in compliance with the ethical policy for animal experiments worldwide [23].

Flow Cytometry

1.5 × 10⁵ cells were incubated overnight in a 6-well culture plate and then incubated in fresh medium with 50–200 nM panobinostat and/or 5–20 mM metformin. After 48-hour treatment, they were washed with phosphate-buffered saline (PBS) and harvested by trypsinization. For cell cycle analysis, cells were resuspended in citrate buffer and stained with propidium iodide. For apoptotic cell analysis, cells were stained with annexin V and 7-aminoactinomycin D (7-AAD) according to the manufacturer's protocol (Beckman Coulter, Marseille, France). They were analyzed by flow cytometry using the CellQuest Pro software (BD Biosciences, San Jose, CA, USA). The experiment was performed three times.

Aggresome Detection

Aggresomes were detected by using PROTEOSTAT aggresome detection kit (Enzo Life Sciences, Farmingdale, NY, USA). Briefly, 1.0 × 10⁵ cells were incubated overnight in 2-well chamber slides before being treated with 200 nM panobinostat and/or 20 mM metformin for 48 hours. Cells were then fixed, permeabilized and

incubated with Hoechst 33342 and PROTEOSTAT dye according to the manufacturer's instructions. Aggresomes and the nucleus were then visualized using a fluorescence microscope (Carl Zeiss, Oberkochen, Germany).

Western Blotting

Cells were treated under the indicated conditions for 48 hours and whole-cell lysates were obtained using a radioimmunoprecipitation assay (RIPA) buffer. Equal amount of proteins were separated by 12.5% sodium dodecyl sulfate-polyacrylamide gel electrophoresis and transferred to nitrocellulose membranes. To evaluate the changes in the expression of proteins in the detergent-insoluble fraction (pellets obtained after the protein extraction using RIPA buffer) induced by each treatment, the pellets were washed with PBS, lysed using the

Table 3. Combination indexes (CIs) for the combination of 5–10 μM suberoylanilide hydroxamic acid (SAHA) and 5–20 mM metformin in bladder cells. CI <1 indicates synergy.

SAHA (μM)	Metformin (mM)		
	5	10	20
UMUC3			
5	0.543	0.482	0.606
10	0.231	0.288	0.389
J82			
5	0.194	0.158	0.306
10	0.677	0.214	0.175
T24			
5	0.902	0.295	0.203
10	0.452	0.222	0.154

Table 2. Combination indexes (CIs) for the combination of 50–200 nM panobinostat and 1–20 mM metformin in bladder cells. CI <1 indicates synergy.

Panobinostat (nM)	Metformin (mM)		
	5	10	20
UMUC3			
100	0.549	0.56	0.277
200	0.608	0.469	0.273
J82			
100	0.661	0.566	0.365
200	0.608	0.447	0.245
T24			
50	0.534	0.548	0.252
100	0.652	0.503	0.281
	1	2.5	5
MBT-2			
100	1.29	0.92	0.91
200	1.26	0.97	0.68

Table 4. Combination indexes (CIs) for the combination of 5–10 μM entinostat and 5–20 mM metformin in bladder cells. CI <1 indicates synergy.

Entinostat (μM)	Metformin (mM)		
	5	10	20
UMUC3			
5	0.097	0.163	0.174
10	0.096	0.146	0.118
J82			
5	0.876	0.826	1.04
10	0.707	0.72	0.756
T24			
5	0.708	0.723	0.669
10	0.723	0.616	0.708

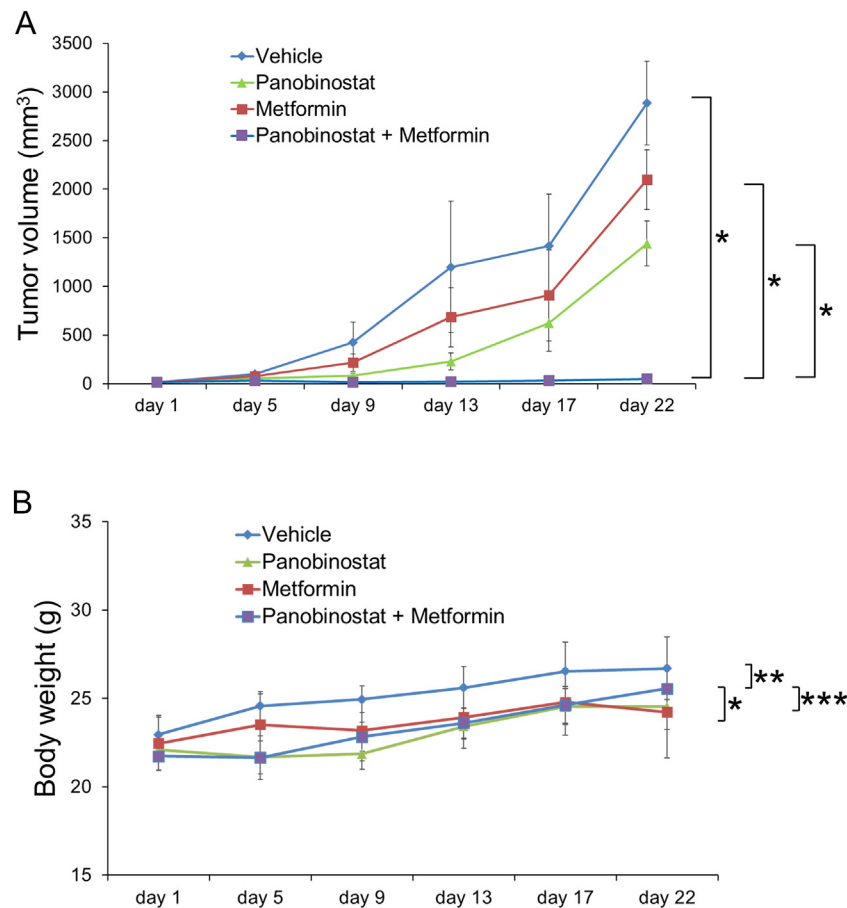


Figure 3. The combination of panobinostat and metformin significantly inhibited bladder cancer growth in murine subcutaneous allograft tumor models. (A) Changes in the tumor volume. A murine allograft model was established using MBT-2 cells. The vehicle group received intraperitoneal injections of dimethyl sulfoxide and distilled water, the treatment groups received 2 mg/kg panobinostat or 100 mg/kg metformin or both. The injections were given once a day for 20 days (10 days on, 2 days off and 10 days on). Mean \pm SE, $n = 5$. $*P = .001$ at day 22. (B) Changes in the body weight. Mean \pm SD, $n = 5$. $*P = .571$, $**P = .413$, $***P = .191$ at day 22.

extraction buffer in the EzSubcell Extract kit (ATTO, Tokyo, Japan) and then subjected to western blotting as described previously [24]. After the membranes were blocked with 5% skimmed milk, they were incubated overnight with a 1:400 dilution of anti-cyclin D1, anti-cyclin dependent kinase (CDK) 4, anti-glucose-regulated protein (GRP) 78, anti-HDAC1, anti-HDAC3 and anti-HDAC6 (Santa Cruz Biotechnology, Santa Cruz, CA, USA); a 1:1000 dilution of anti-acetyl CoA carboxylase (ACC), anti-phospho-AMPK (p-AMPK), anti-AMPK, anti-phospho-ribosomal protein S6 (p-S6), anti-S6, anti-phospho-eukaryotic translation initiation factor 4E-binding protein 1 (p-4EBP1), anti-4EBP1 and anti-endoplasmic reticulum resident protein (ERp) 44 (Cell Signaling Technology, Danvers, MA, USA); a 1:2000 dilution of anti-acetyl lysine (Cusabio, Houston, TX, USA); and a 1:5000 dilution of anti-acetylated histone (Abcam, Cambridge, UK), anti-acetylated α -tubulin (Enzo Life Sciences, Farmingdale, NY, USA) and anti-actin (Millipore, Billerica, MA, USA). The membranes were then incubated with horseradish-tagged secondary antibodies (Bio-Rad, Hercules, CA, USA). The bands were visualized by chemiluminescence with the ECL Plus system (GE Healthcare, Wauwatosa, WI, USA) according to the manufacturer's instructions.

Statistical Analysis

Combination indexes were calculated by the Chou and Talalay method using CalcuSyn software (Biosoft, Cambridge, UK) [25].

The statistical significance of differences was determined using the Mann-Whitney U test (JMP pro14 software; SAS Institute, Cary, NC, USA), and P values less than .05 were considered to indicate a significant difference.

Results

Panobinostat Induced Histone Acetylation and Endoplasmic Reticulum (ER) Stress But Also Activated the mTOR Pathway

Panobinostat inhibited the growth of bladder cancer cells in a dose-dependent manner (Figure 1A), and the mean inhibitory concentration (IC₅₀) varied among cell lines (Table 1). As expected, panobinostat induced histone acetylation in a dose-dependent manner (Figure 1B). Because inhibition of HDACs reportedly suppresses molecular chaperones and induces ER stress [26,27], we also examined whether panobinostat induced ER stress in bladder cancer cells. Panobinostat increased the expression of the ER stress markers GRP78 and ERp44, showing that it induced ER stress as well as histone acetylation. It also decreased the expression of phosphorylated 4EBP1, indicating that it inhibited one of the downstream proteins of the mTOR pathway. Interestingly, panobinostat also increased the phosphorylation of S6, another downstream protein of the mTOR pathway located at a different signaling axis from 4EBP1. While suppressing one signaling axis of the mTOR pathway,

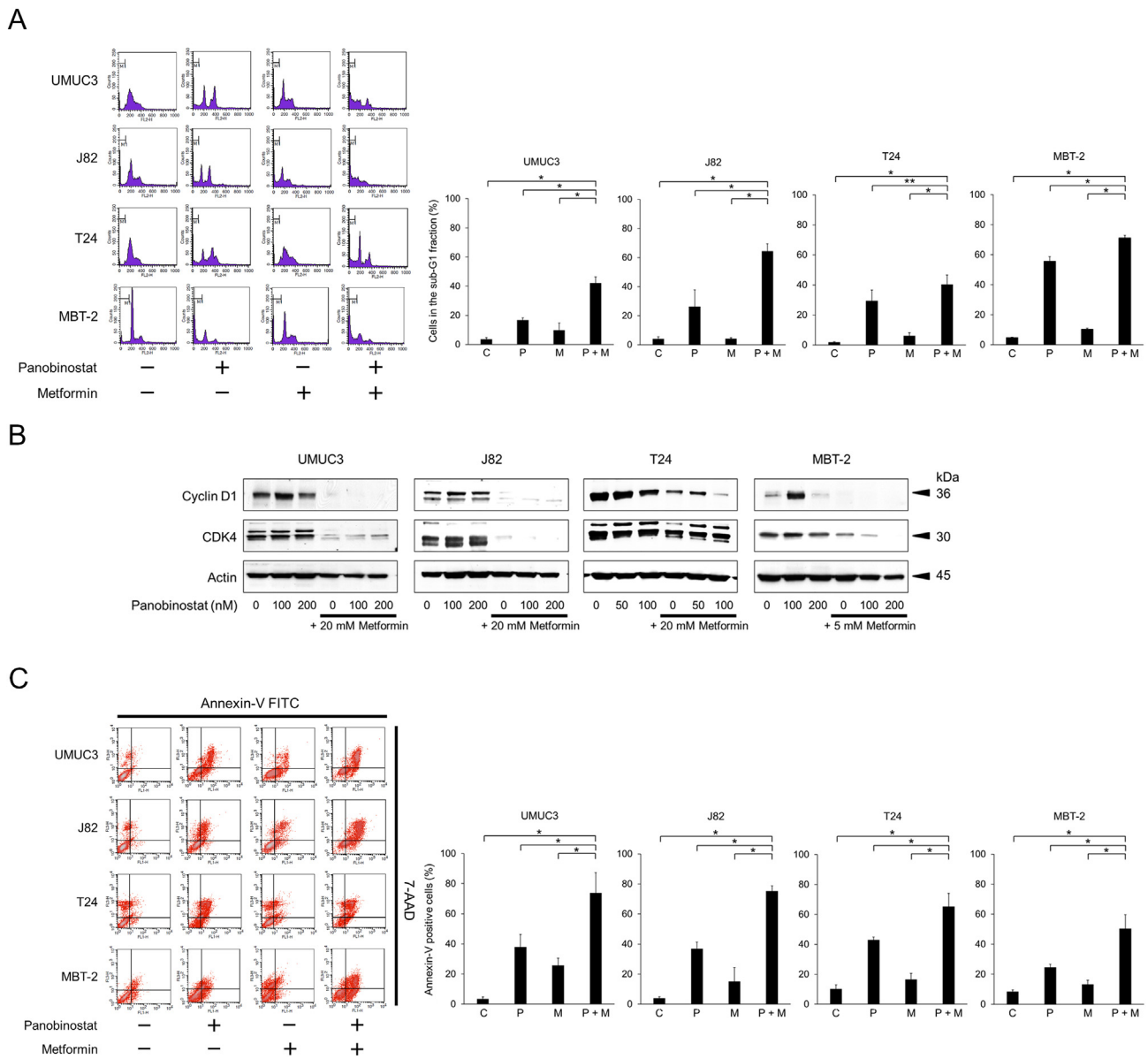


Figure 4. The combination of panobinostat and metformin induced robust apoptosis. (A) Cell cycle analysis. Cells were treated for 48 hours with 100–200 nM panobinostat and/or 5–20 mM metformin. Changes in the cell cycle were evaluated using flow cytometry. 10,000 cells were counted. Bar graphs show the percentages of the cells in the sub-G1 fraction. Data are expressed as mean \pm SD from three independent experiments. C, control; P, panobinostat (200 nM in UMC3, J82, and MBT-2 cells; 100 nM in T24 cells); M, metformin (20 mM in UMC3, J82, and T24 cells; 5 mM in MBT-2 cells). * $P = .0495$, ** $P = .126$. (B) Western blotting for cyclin D1 and cyclin-dependent kinase (CDK) 4. Cells were treated for 48 hours with 50–200 nM panobinostat and/or 5–20 mM metformin. Actin was used for the loading control. Representative blots are shown. (C) Annexin-V assay. Cells were treated for 48 hours with 100–200 nM panobinostat and/or 5–20 mM metformin. Apoptotic cells were detected by annexin-V assay using flow cytometry. 10,000 cells were counted. Bar graphs show the percentages of annexin-V positive cells. Data are expressed as mean \pm SD from three independent experiments. FITC, fluorescein isothiocyanate; 7-AAD, 7-amino-actinomycin D; C, control; P, panobinostat (200 nM in UMC3, J82, and MBT-2 cells; 100 nM in T24 cells); M, metformin (20 mM in UMC3, J82, and T24 cells; 5 mM in MBT-2 cells). * $P = .0495$.

panobinostat was shown to activate another signaling pathway and thereby attenuate its anticancer activity.

The Combination of Panobinostat and Metformin Inhibited Bladder Cancer Growth Both In Vitro and In Vivo

The combination of panobinostat and metformin inhibited the growth of bladder cancer cells effectively (Figure 2A). The combined cytotoxic effects were also apparent in morphology. On microscopic

examination, cells treated by the combination had a round and swollen morphology and most of them were floating and markedly different from the untreated cells (Figure 2B). Furthermore, isobologram analysis and calculation of the combination index confirmed the synergism of this combination (Figure 2C and Table 2).

To confirm the beneficial combined effect of an HDAC inhibitor and metformin, we then treated the bladder cancer cells with other HDAC inhibitors, SAHA or entinostat, in combination with metformin.

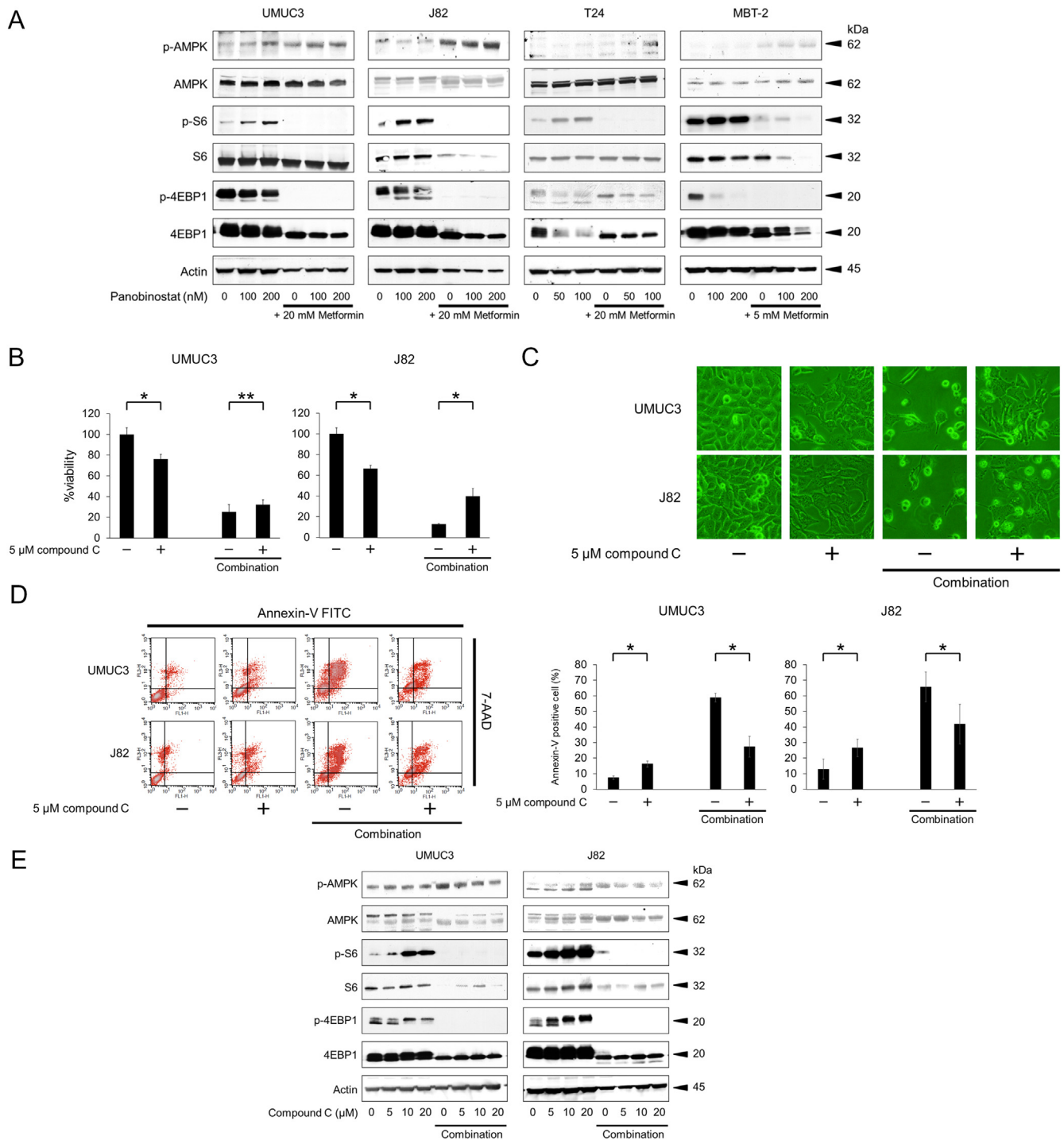


Figure 5. Metformin activated AMP-activated protein kinase (AMPK) and inhibited the panobinostat-activated mammalian target of rapamycin pathway. (A) Western blotting for AMPK, S6 ribosomal protein (S6), and eukaryotic translation initiation factor 4E-binding protein 1 (4EBP1). Cells were treated with 50–200 nM panobinostat and/or 5–20 mM metformin for 48 hours. Actin was used for the loading control. Representative blots are shown. (B) MTS assay. Cells were treated with 200 nM panobinostat and 20 mM metformin with or without 5 μ M compound C for 48 hours. Bars represent mean \pm SD, $n = 12$. $*P = .0007$, $**P = .0114$. (C) Photomicrographs after 48-hour treatment. Cells were treated with 200 nM panobinostat and 20 mM metformin with or without 5 μ M compound C for 48 hours. Original magnification, 200 \times . (D) Annexin-V assay. Cells were treated with 200 nM panobinostat and 20 mM metformin with or without 5 μ M compound C for 48 hours. Apoptotic cells were detected by annexin-V assay using flow cytometry. 10,000 cells were counted. Bar graphs show the percentages of annexin-V positive cells. Data are expressed as mean \pm SD from three independent experiments. FITC, fluorescein isothiocyanate; 7-AAD, 7-amino-actinomycin D. $*P = .0495$. (E) Western blotting for AMPK, S6, and 4EBP1. Cells were treated for 48 hours with 200 nM panobinostat and 20 mM metformin with or without 5–20 μ M compound C. Actin was used for the loading control. Representative blots are shown.

Interestingly, we found that these combinations also inhibited bladder cancer growth synergistically (Figure 2, D and E and Tables 3 and 4). Combining an HDAC inhibitor and metformin was thus shown to be a promising approach to killing bladder cancer cells.

We then investigated whether the combination of panobinostat and metformin affected the clonogenic survival of bladder cancer cells. The combination of panobinostat and metformin inhibited their colony formation significantly (Figure 2F). Thus the combination was shown to inhibit bladder cancer growth effectively *in vitro*. We next tested the *in vivo* efficacy of the combination. In murine subcutaneous allograft tumor models using MBT-2 cells, a 22-day treatment using the combination of panobinostat and metformin was well-tolerated and almost completely suppressed tumor growth (Figure 3A). No remarkable treatment-associated adverse events were observed and changes in body weight did not significantly differ among the groups (Figure 3B), reflecting the safety of this combination therapy. Thus the combination of panobinostat and metformin was shown to inhibit bladder cancer cell growth effectively both *in vitro* and *in vivo*.

The Combination of Panobinostat and Metformin Induced Robust Apoptosis

We evaluated the cell cycle changes induced by the combination of panobinostat and metformin. In all the cell lines, the combination increased the number of the cells in sub-G1 fraction significantly (Figure 4A). Western blotting demonstrated that it markedly decreased the expression of the cell-cycle regulators cyclin D1 and CDK4 (Figure 4B), which was consistent with the cell cycle changes it induced. The combination also increased the number of annexin-V positive cells significantly (Figure 4C). Thus the combination of panobinostat and metformin was shown to induce robust apoptosis.

Metformin Activated AMPK and Inhibited the Panobinostat-Activated mTOR Pathway

We postulated that metformin in the combination would activate AMPK and thereby inhibit the panobinostat-activated mTOR pathway, enhancing panobinostat's anticancer activity, so we evaluated combination-induced changes in the expression of AMPK and mTOR-related proteins. In all the cell lines, metformin increased the phosphorylation of AMPK and decreased the panobinostat-caused phosphorylation of S6, demonstrating that metformin actually inhibited the panobinostat-activated mTOR pathway (Figure 5A). Furthermore, the panobinostat-caused dephosphorylation of 4EBP1 was further promoted by metformin, which also attested that metformin inhibited mTOR.

To further evaluate the role of AMPK activation in the combination's action, we treated bladder cancer cells with the AMPK inhibitor compound C with and without the panobinostat-metformin combination. Compound C significantly attenuated the combination's cytotoxic effect (Figure 5, B and C). It also decreased the combination-increased annexin-V positive cells significantly, showing that it inhibited the combination-induced apoptosis (Figure 5D). These results suggest that AMPK activation plays an important role in the combination's anticancer effect. To explore the relevance of AMPK phosphorylation, we treated the cells with different concentrations of compound C with and without the combination and evaluated changes in the expression of mTOR-related proteins. Western blotting showed that compound C increased the phosphorylation of both S6 and 4EBP1 in a dose-

dependent manner, confirming that it actually inhibited the function of AMPK and thereby activated the mTOR pathway (Figure 5E). The combination of panobinostat and metformin increased the expression of phosphorylated AMPK as it did in the previous experiment and decreased the compound-C activated phosphorylation of S6 and 4EBP1. Thus AMPK phosphorylation was shown to be an important mechanism by which the combination activated AMPK and inhibited the mTOR pathway. It is interesting that compound C decreased the combination-increased phosphorylated AMPK expression only slightly, suggesting that suppressing activated AMPK kinase was not the only way that compound C inhibited AMPK function.

The Combination of Panobinostat and Metformin Induced Protein Acetylation Cooperatively

AMPK activation reportedly induces histone acetylation in other cancers [20,21], so we postulated that the combination of panobinostat and metformin would cooperatively induce histone acetylation. The AMPK activator AICAR increased phosphorylation of AMPK and induced acetylation of histone and α -tubulin (Figure 6A). Thus AMPK activation was shown to induce protein acetylation also in bladder cancer cells. The combination of panobinostat and metformin decreased the expression of ACC but did not always induce protein acetylation as postulated (Figure 6B): metformin enhanced panobinostat-induced histone acetylation only in UMUC3 and MBT-2 cells and, surprisingly, decreased it in J82 and T24 cells. Panobinostat-induced α -tubulin acetylation was promoted by metformin in T24 cells but was decreased by it in UMUC3, J82 and MBT-2 cells. As with the whole protein, no cooperative acetylation of lysine was seen by the combination. These results were inconsistent with our postulation and we thought that some of the acetylated proteins might shift to the detergent-insoluble fraction. We therefore solubilized the detergent-insoluble fraction and subjected the newly obtained lysates to western blotting. The combination of panobinostat and metformin induced the acetylation of histone, α -tubulin and whole protein contained in the detergent-insoluble fraction cooperatively in all the cell lines (Figure 6C). Interestingly, the acetylation was especially notable in the cell lines in which protein acetylation in the detergent-soluble fraction was decreased. Thus the combination was shown to induce protein acetylation cooperatively.

To further explore the mechanism of this cooperative protein acetylation, we evaluated changes in the expression of HDACs, enzymes that deacetylate proteins. We found that the combination of panobinostat and metformin decreased the expression of HDACs (Figure 6D), especially HDAC6, and this decreased HDAC expression, like the combination's AMPK activation, is a mechanism by which the combination enhanced protein acetylation.

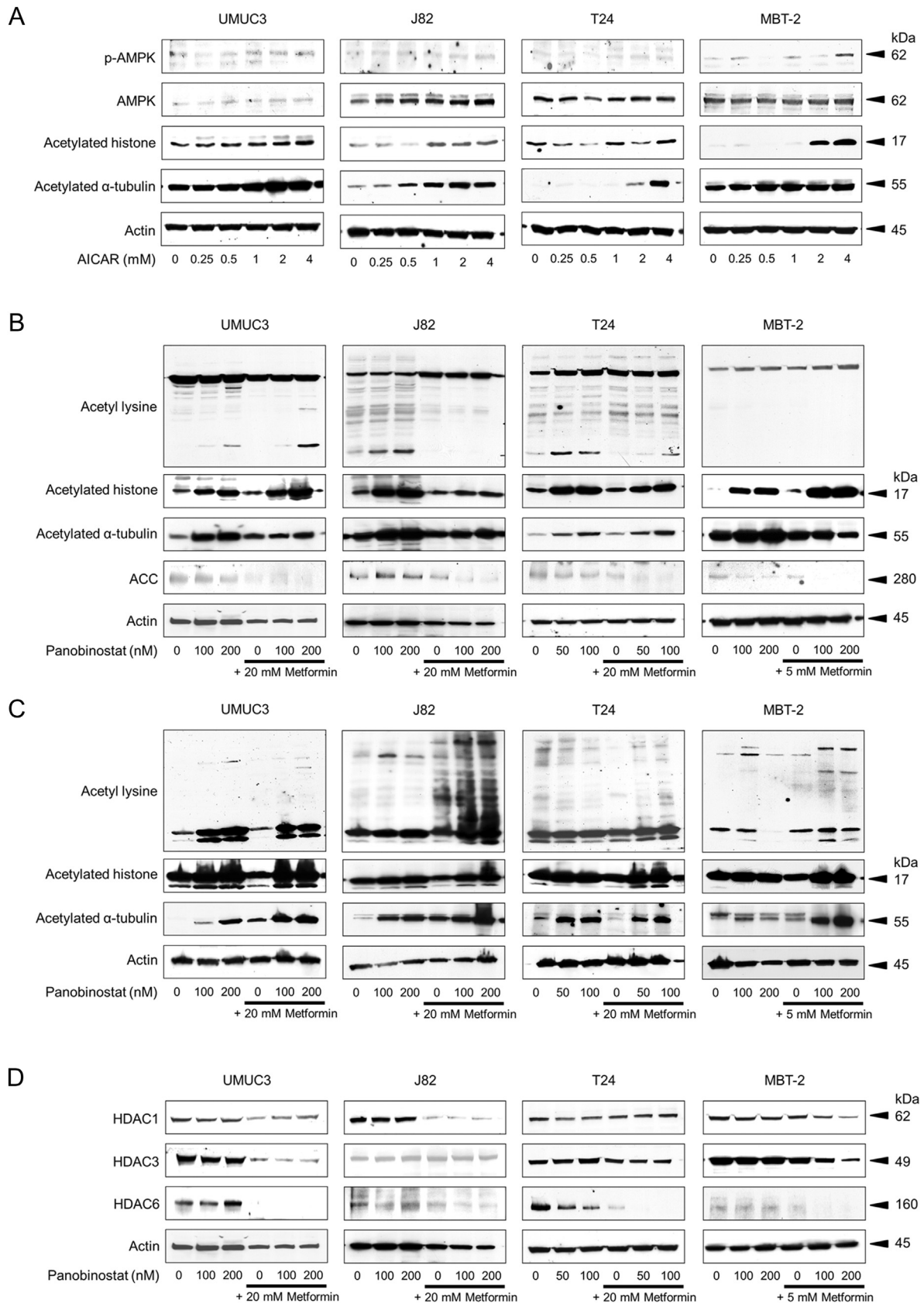
The Combination of Panobinostat and Metformin Induced ER Stress

Because the combination of panobinostat and metformin decreased the expression of HDACs, we thought that it would induce ER stress cooperatively. In UMUC3 and J82 cells the combination increased the expression of ERp44 cooperatively, and in T24 and MBT-2 cells it increased the expression of GRP78 cooperatively (Figure 7A). Thus the combination increased the expression of the ER stress markers, showing that it actually induced ER stress in bladder cancer cells. Furthermore, compound C attenuated the combination-induced histone acetylation and ER

stress (Figure 7B), confirming that AMPK activation was one important mechanism of this ER stress induction.

Generally, ER stress is induced in response to increased unfolded proteins in the cell [28] and some of the accumulated unfolded proteins

then aggregate and form aggresomes [29,30]. We therefore then examined whether the combination caused aggresome formation. Either panobinostat or metformin alone caused aggresome formation moderately and the combination did so extensively (Figure 7C). This



aggresome formation was consistent with our observation that combination-induced protein acetylation was especially notable in the detergent-insoluble fraction (*i.e.*, some of the acetylated proteins aggregated and shifted to the detergent-insoluble fraction).

Discussion

Dysregulation of HDAC is associated with tumorigenicity and the survival of malignant cells [31–33]. HDAC inhibitors have therefore been attracting attention as novel anticancer drugs [33–35]. In the present study the pan-HDAC inhibitor panobinostat induced histone acetylation but also activated the mTOR pathway by causing phosphorylation of S6, which could be attributed to drug resistance and limited efficacy [11–13]. We therefore thought that combining panobinostat with a drug that suppresses the mTOR pathway would enhance panobinostat's anticancer activity.

The mTOR pathway is also an attracting target for bladder cancer treatment. Genetic variations in phosphatidylinositol 3-kinase-mTOR pathway have been reported to be associated with bladder cancer risk [36] and correlate with higher grades and higher stages [37]. Furthermore, it has been shown that PI3K-mTOR dual inhibitor NVP-BEZ235 suppresses bladder cancer cell proliferation *in vitro* and *in vivo* [38] and that mTOR inhibitors inhibit bladder cancer cell viability by suppressing mTOR-related proteins such as p-S6 and p-4EBP1 [39,40]. Nonetheless, the mTOR inhibitor temsirolimus was not effective in phase II trials in patients with metastatic urothelial cancer [41]. AMPK is a metabolic sensor and has been demonstrated to be potentially useful for treating cancer by suppressing the mTOR pathway [14–17]. Downregulation of AMPK has been reported in many malignancies, including bladder cancer [42–46], and our study showed that the AMPK activator AICAR inhibited the growth of bladder cancer cells (Figure S1). Metformin has been attracting attention for cancer prevention and therapy by activating AMPK and decreasing ATP production by inhibiting mitochondrial respiratory chain complex I [18,19]. We showed in the present study that metformin indeed augmented panobinostat's activity by activating AMPK and suppressing panobinostat-induced mTOR activation. We also showed that this AMPK activation was an important mechanism of the combination's action because the AMPK inhibitor compound C attenuated the combination's cytotoxicity and ability to induce apoptosis.

The combination of panobinostat and metformin also induced protein acetylation cooperatively. In addition to suppressing mTOR activation, AMPK inhibits ACC, an enzyme that causes cellular acetyl-CoA to accumulate and thereby enhances histone acetylation [20–22]. In our study the combination of panobinostat and metformin also decreased the expression of ACC and enhanced panobinostat-induced protein acetylation. Histone acetylation is a well-known anticancer mechanism [7,8], and α -tubulin acetylation

also acts against cancer because it stabilizes microtubules and thereby suppresses epithelial mesenchymal transition, one of the hallmarks of cancer progression [47]. The whole protein acetylation suggested that the histone-acetylation-related molecules in the cell, such as HDACs and ACC, targeted not only histone but also non-histone proteins. Interestingly, the protein acetylation induced by the combination was especially notable in the detergent-insoluble fraction. Several prior studies have found that misfolded protein accumulation leads to induction of ER stress, resulting in protein aggregation and shifting to the detergent-insoluble fraction [24,30,48]. We have shown in the present study that the combination also caused ER stress and aggresome formation. Protein acetylation may therefore play a role in the protein aggregation process.

ER stress induction is beneficial approach for killing cancer [49,50]. ER stress is induced when the amount of misfolded protein exceeds the capacity of the ER refolding capacity, and prolonged ER stress kills cancer cells [51]. We have previously reported that ER stress had multiple effects—such as HDAC inhibition [24,52,53], mTOR suppression [22,54] and tumor necrosis factor-related apoptosis-inducing ligand (TRAIL) receptor upregulation [55]—and killed urological cancer cells effectively [24,52–56]. In the present study the combination of panobinostat and metformin induced ER stress cooperatively, and this would be an important mechanism of the combination's anticancer action.

To the best of our knowledge this is the first study to investigate the interaction of panobinostat and metformin in cancer cells, but it has some limitations. Because the combination suppressed *in vivo* tumor growth almost completely, we could not obtain the tumor specimens and therefore could not assess changes in protein expression and histopathological findings *in vivo*. Another limitation is that the role of the whole protein acetylation was unknown. As mentioned above, it may play a role in the protein aggregation process, and acetylation itself may cause proteins to aggregate. On the other hand, the HDAC suppression may inhibit molecular chaperones such as HSP90 [57], increasing misfolded proteins and thereby causing aggregation, and the whole protein acetylation may be only a result of the HDAC suppression and make no contribution to protein aggregation. Clarifying the exact role of the whole protein acetylation would be an important next step.

Combinations of an HDAC inhibitor and metformin have already been studied in other types of cancer [58–60], but in the present study using bladder cancer cells we have found novel mechanisms of action of the combination of the HDAC inhibitor panobinostat and metformin. A possible mechanism of action of the combination of panobinostat and metformin is summarized in Figure 8. Metformin augmented panobinostat's antineoplastic activity in bladder cancer cells by activating AMPK. Inducing histone and non-histone acetylation and ER stress would also

Figure 6. The combination of panobinostat and metformin induced protein acetylation cooperatively. (A) Western blotting for AMP-activated protein kinase (AMPK), acetylated histone, and acetylated α -tubulin. Cells were treated for 48 hours with 0.25–4 mM of the AMPK activator 5-aminoimidazole-4-carboxamide (AICAR). Actin was used for the loading control. Representative blots are shown. (B) Western blotting for acetyl lysine, acetylated histone, acetylated α -tubulin, and acetyl CoA carboxylase (ACC). Cells were treated for 48 hours with 50–200 nM panobinostat and/or 5–20 mM metformin. Actin was used for the loading control. Representative blots are shown. (C) Western blotting for acetyl lysine, acetylated histone, and acetylated α -tubulin in the detergent-insoluble fraction. Cells were treated for 48 hours with 50–200 nM panobinostat and/or 5–20 mM metformin and the detergent-insoluble fraction was lysed and subjected to western blotting. Actin was used for the loading control. Representative blots are shown. (D) Western blotting for histone deacetylase (HDAC) 1, 3, and 6. Cells were treated for 48 hours with 50–200 nM panobinostat and/or 5–20 mM metformin. Actin was used for the loading control. Representative blots are shown.

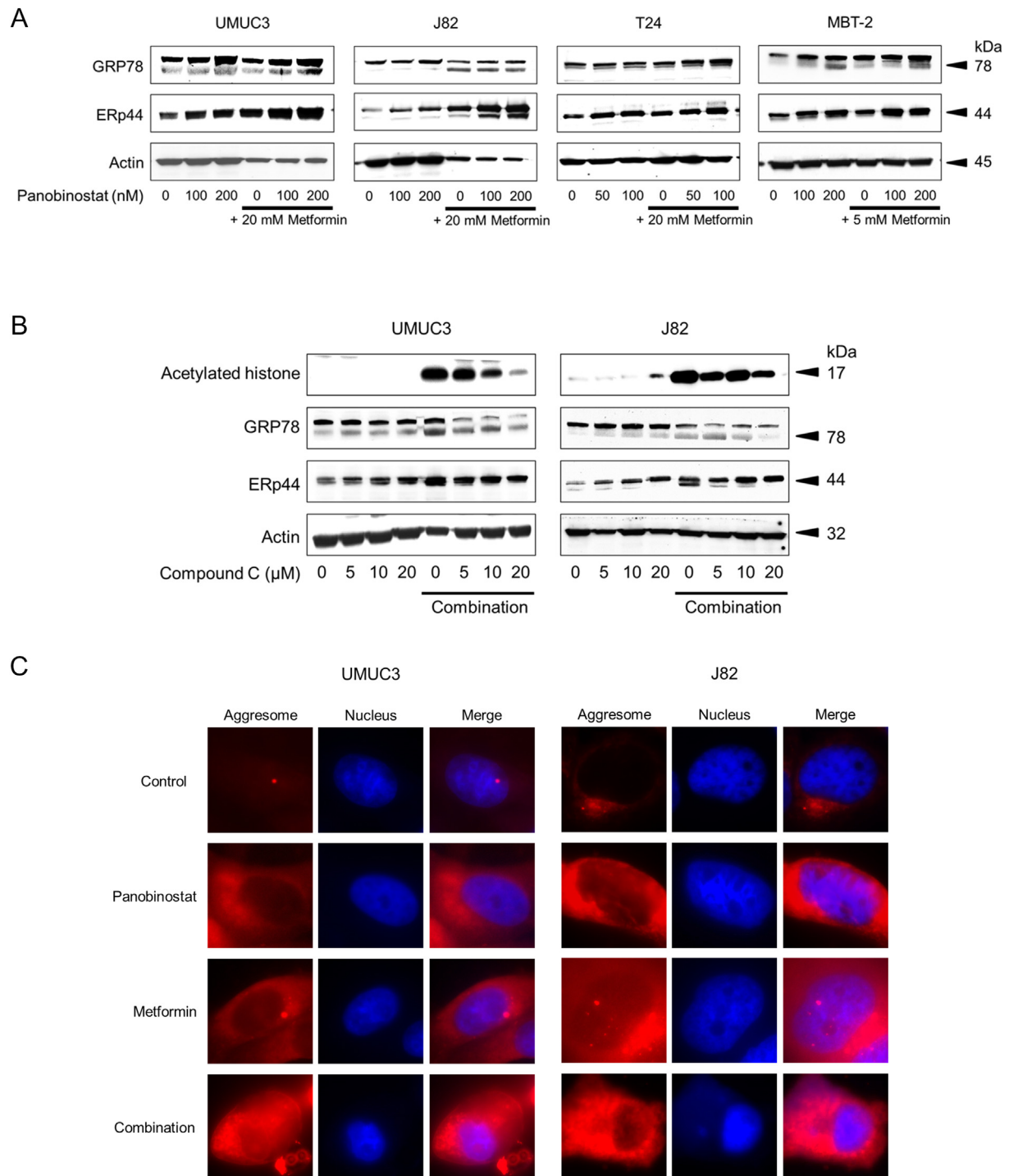


Figure 7. The combination of panobinostat and metformin induced endoplasmic reticulum (ER) stress. (A) Western blotting for the ER stress markers glucose-regulated protein (GRP) 78 and endoplasmic reticulum resident protein (ERp) 44. Cells were treated for 48 hours with 50–200 nM panobinostat and/or 5–20 mM metformin. Actin was used for the loading control. Representative blots are shown. (B) Western blotting for the acetylated histone, GRP78, and ERp44. Cells were treated for 48 hours with 200 nM panobinostat and 20 mM metformin and/or 5–20 μ M compound C. Actin was used for the loading control. Representative blots are shown. (C) Aggresome detection after 48-hour treatment with 200 nM panobinostat and/or 20 mM metformin. Red, aggresome; blue, nucleus. Original magnification, 1000 \times .

be important mechanisms of action. Because both drugs have been widely used clinically, it would be relatively easy to translate our results into clinical use. The present study would provide a basis for testing this combination in patients with advanced bladder cancer.

Supplementary data to this article can be found online at <https://doi.org/10.1016/j.tranon.2019.02.001>.

Acknowledgements

None.

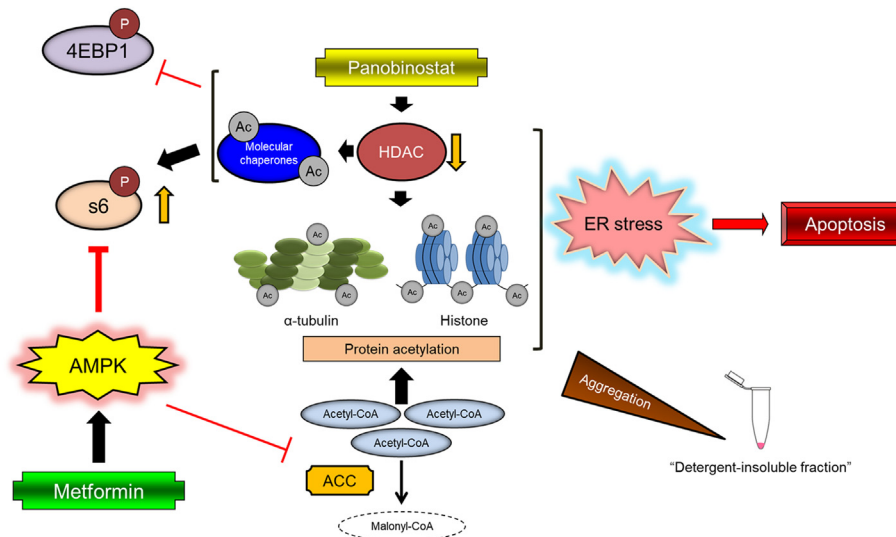


Figure 8. A possible mechanism of action of the combination of panobinostat and metformin.

Ethical Standards

All applicable international, national, and institutional guidelines for the care and use of animals were followed.

References

- Allareddy V, Kennedy J, West M, and Konety B (2006). Quality of life in long-term survivors of bladder cancer. *Cancer* **106**, 2355–2362.
- von der Maase H, Sengelov L, Roberts JT, Ricci S, Dogliotti L, Oliver T, Moore MJ, Zimmermann A, and Arning M (2005). Long-term survival results of a randomized trial comparing gemcitabine plus cisplatin, with methotrexate, vinblastine, doxorubicin, plus cisplatin in patients with bladder cancer. *J Clin Oncol* **23**, 4602–4608.
- Rosenberg JE, Carroll PR, and Small EJ (2005). Update on chemotherapy for advanced bladder cancer. *J Urol* **174**, 14.
- Bellmunt J, de Wit R, Vaughn DJ, Fradet Y, Lee JL, Fong L, Vogelzang NJ, Climent MA, Petrylak DP, and Choueiri TK, et al (2017). Pembrolizumab as second-line therapy for advanced urothelial carcinoma. *N Engl J Med* **376**, 1015–1026.
- Farina MS, Lundgren KT, and Bellmunt J (2017). Immunotherapy in urothelial cancer: Recent results and future perspectives. *Drugs* **77**, 1077–1089.
- Bellmunt J, Powles T, and Vogelzang NJ (2017). A review on the evolution of PD-1/PD-L1 immunotherapy for bladder cancer: The future is now. *Cancer Treat Rev* **54**, 58–67.
- Bolden JE, Peart MJ, and Johnstone RW (2006). Anticancer activities of histone deacetylase inhibitors. *Nat Rev Drug Discov* **5**, 769–784.
- Dokmanovic M, Clarke C, and Marks PA (2007). Histone deacetylase inhibitors: overview and perspectives. *Mol Cancer Res* **5**, 981–989.
- San-Miguel JF, Hungria VT, Yoon SS, Beksac M, Dimopoulos MA, Elghandour A, Jdrzejczak WW, Günther A, Nakorn TN, and Siritanaratkul N, et al (2014). Panobinostat plus bortezomib and dexamethasone versus placebo plus bortezomib and dexamethasone in patients with relapsed or relapsed and refractory multiple myeloma: a multicentre, randomised, double-blind phase 3 trial. *Lancet Oncol* **15**, 1195–1206.
- Laubach JP, Moreau P, San-Miguel JF, and Richardson PG (2015). Panobinostat for the treatment of multiple myeloma. *Clin Cancer Res* **21**, 4767–4773.
- Hainsworth JD, Infante JR, Spigel DR, Arrowsmith ER, Boccia RV, and Burris HA (2011). A phase II trial of panobinostat, a histone deacetylase inhibitor, in the treatment of patients with refractory metastatic renal cell carcinoma. *Cancer Invest* **29**, 451–455.
- Prince H, Bishton M, and Johnstone R (2009). Panobinostat (LBH589): a potent pan-deacetylase inhibitor with promising activity against hematologic and solid tumors. *Future Oncol* **5**, 601–612.
- Lemoine M, Derenzini E, Buglio D, Medeiros LJ, Davis RE, Zhang J, Ji Y, and Younes A (2012). The pan-deacetylase inhibitor panobinostat induces cell death and synergizes with everolimus in Hodgkin lymphoma cell lines. *Blood* **119**, 4017–4025.
- Faubert B, Vincent E, Poffenberger M, and Jones RG (2015). The AMP-activated protein kinase (AMPK) and cancer: many faces of a metabolic regulator. *Cancer Lett* **356**, 165–170.
- Jeon S and Hay N (2015). The double-edged sword of AMPK signaling in cancer and its therapeutic implications. *Arch Pharm Res* **38**, 346–357.
- Wang W and Guan K (2009). AMP-activated protein kinase and cancer. *Acta Physiol (Oxf)* **196**, 55–63.
- Zadra G, Batista J, and Loda M (2015). Dissecting the dual role of AMPK in cancer: from experimental to human studies. *Mol Cancer Res* **13**, 1059–1072.
- El-Mir M, Nogueira V, Fontaine E, Avéret N, Rigoulet M, and Leverve X (2000). Dimethylbiguanide inhibits cell respiration via an indirect effect targeted on the respiratory chain complex I. *J Biol Chem* **275**, 223–228.
- Owen M, Doran E, and Halestrap A (2000). Evidence that metformin exerts its anti-diabetic effects through inhibition of complex I of the mitochondrial respiratory chain. *Biochem J* **348**, 607–614.
- Vancura A and Vancurova I (2017). Metformin induces protein acetylation in cancer cells. *Oncotarget* **8**, 39939–39940.
- Zhang M, Galdieri L, and Vancura A (2013). The yeast AMPK homolog SNF1 regulates acetyl coenzyme A homeostasis and histone acetylation. *Mol Cell Biol* **33**, 4701–4717.
- Galdieri L and Vancura A (2012). Acetyl-CoA carboxylase regulates global histone acetylation. *J Biol Chem* **287**, 23865–23876.
- Workman P, Aboagye EO, Balkwill F, Balmain A, Bruder G, Chaplin DJ, Double JA, Everitt J, Farningham DA, and Glennie MJ, et al (2010). Committee of the National Cancer Research Institute. Guidelines for the welfare and use of animals in cancer research. *Br J Cancer* **102**, 1555–1577.
- Sato A, Asano T, Okubo K, Isono M, and Asano T (2017). Ritonavir and ixazomib kill bladder cancer cells by causing ubiquitinated protein accumulation. *Cancer Sci* **108**, 1194–1202.
- Chou TC (2010). Drug combination studies and their synergy quantification using the Chou-Talalay method. *Cancer Res* **70**, 440–446.
- Baumeister P, Dong D, Fu Y, and Lee AS (2009). Transcriptional induction of GRP78/BiP by histone deacetylase inhibitors and resistance to histone deacetylase inhibitor-induced apoptosis. *Mol Cancer Ther* **8**, 1086–1094.
- Rao R, Nalluri S, Kolhe R, Yang Y, Fiskus W, Chen J, Ha K, Buckley KM, Balusu R, and Coothankandaswamy V, et al (2010). Treatment with panobinostat induces glucose-regulated protein 78 acetylation and endoplasmic reticulum stress in breast cancer cells. *Mol Cancer Ther* **9**, 942–952.
- Kaufman RJ (1999). Stress signaling from the lumen of the endoplasmic reticulum: coordination of gene transcriptional and translational controls. *Genes Dev* **13**, 1211–1233.
- Johnston JA, Ward CL, and Kopito RR (1998). Aggresomes: a cellular response to misfolded proteins. *J Cell Biol* **143**, 1883–1898.

- [30] Nawrocki ST, Carew JS, Pino MS, Highshaw RA, Andrtbacka RH, Dunner Jr K, Pal A, Bornmann WG, Chiao PJ, and Huang P, et al (2006). Aggresome disruption: a novel strategy to enhance bortezomib-induced apoptosis in pancreatic cancer cells. *Cancer Res* **66**, 3773–3781.
- [31] Spange S, Wagner T, Heinzel T, and Krämer OH (2009). Acetylation of non-histone proteins modulates cellular signalling at multiple levels. *Int J Biochem Cell Biol* **41**, 185–198.
- [32] Wade PA (2001). Transcriptional control at regulatory checkpoints by histone deacetylases: molecular connections between cancer and chromatin. *Hum Mol Genet* **10**, 693–698.
- [33] Gallinari P, Di Marco S, Jones P, Pallaoro M, and Steinkühler C (2007). HDACs, histone deacetylation and gene transcription: from molecular biology to cancer therapeutics. *Cell Res* **17**, 195–211.
- [34] Carew JS, Giles FJ, and Nawrocki ST (2008). Histone deacetylase inhibitors: mechanisms of cell death and promise in combination cancer therapy. *Cancer Lett* **269**, 7–17.
- [35] Huang H, Reed CP, Zhang JS, Shridhar V, Wang L, and Smith DI (1999). Carboxypeptidase A3 (CPA3): A novel gene highly induced by histone deacetylase inhibitors during differentiation of prostate epithelial cancer cells. *Cancer Res* **59**, 1981–1988.
- [36] Chen M, Cassidy A, Gu J, Delclos GL, Zhen F, Yang H, Hildebrandt MA, Lin J, Ye Y, and Chamberlain RM, et al (2009). Genetic variations in PI3K-AKT-mTOR pathway and bladder cancer risk. *Carcinogenesis* **30**, 2047–2052.
- [37] Hansel DE, Platt E, Orloff M, Harwalker J, Sethu S, Hicks JL, De Marzo A, Steinle RE, Hsi ED, and Theodorescu D, et al (2010). Mammalian target of rapamycin (mTOR) regulates cellular proliferation and tumor growth in urothelial carcinoma. *Am J Pathol* **176**, 3062–3072.
- [38] Matsushima M, Kikuchi E, Matsumoto K, Hattori S, Takeda T, Kosaka T, Miyajima A, and Oya M (2015). Intravesical dual PI3K/mTOR complex 1/2 inhibitor NVP-BEZ235 therapy in an orthotopic bladder cancer model. *Int J Oncol* **47**, 377–383.
- [39] Chiong E, Lee IL, Dadbin A, Sabichi AL, Harris L, Urbauer D, McConkey DJ, Dickstein RJ, Cheng T, and Grossman HB (2011). Effects of mTOR inhibitor everolimus (RAD001) on bladder cancer cells. *Clin Cancer Res* **17**, 2863–2873.
- [40] Fechner G, Classen K, Schmidt D, Hauser S, and Müller SC (2009). Rapamycin inhibits in vitro growth and release of angiogenic factors in human bladder cancer. *Urology* **73**, 665–669.
- [41] Gerullis H, Eimer C, Ecke TH, Georgas E, Freitas C, Kastenholz S, Arndt C, Heusch C, and Otto T (2012). A phase II trial of temsirolimus in second-line metastatic urothelial cancer. *Med Oncol* **29**, 2870–2876.
- [42] Hadad SM, Baker L, Quinlan PR, Robertson KE, Bray SE, Thomson G, Kellock D, Jordan LB, Purdie CA, and Hardie DG, et al (2009). Histological evaluation of AMPK signaling in primary breast cancer. *BMC Cancer* **9**, 307.
- [43] Zheng L, Yang W, Wu F, Wang C, Yu L, Tang L, Qiu B, Li Y, Guo L, and Wu M, et al (2013). Prognostic significance of AMPK activation and therapeutic effects of metformin in hepatocellular carcinoma. *Clin Cancer Res* **19**, 5372–5380.
- [44] Fox MM, Phoenix KN, Kopsiaftis SG, and Claffey KP (2013). AMP-activated protein kinase alpha 2 isoform suppression in primary breast cancer alters AMPK growth control and apoptotic signaling. *Genes Cancer* **4**, 3–14.
- [45] Kim YH, Liang H, Liu X, Lee JS, Cho JY, Cheong JH, Kim H, Li M, Downey TJ, and Dyer MD, et al (2012). AMPK alpha modulation in cancer progression: multilayer integrative analysis of the whole transcriptome in Asian gastric cancer. *Cancer Res* **72**, 2512–2521.
- [46] Kopsiaftis S, Hegde P, Taylor III JA, and Claffey KP (2016). AMPK α is suppressed in bladder cancer through macrophage-mediated mechanisms. *Transl Oncol* **9**, 606–616.
- [47] Gu S, Liu Y, Zhu B, Ding K, Yao TP, Chen F, Zhan L, Xu P, Ehrlich M, and Liang T, et al (2016). Loss of α -Tubulin acetylation is associated with TGF- β -induced epithelial-mesenchymal transition. *J Biol Chem* **291**, 5396–5405.
- [48] Mimnaugh EG, Xu W, Vos M, Yuan X, Isaacs JS, Bisht KS, Gius D, and Neckers L (2004). Simultaneous inhibition of hsp 90 and the proteasome promotes protein ubiquitination, causes endoplasmic reticulum-derived cytosolic vacuolization, and enhances antitumor activity. *Mol Cancer Ther* **3**, 551–566.
- [49] Liu Y and Ye Y (2011). Proteostasis regulation at the endoplasmic reticulum: a new perturbation site for targeted cancer therapy. *Cell Res* **21**, 867–883.
- [50] Ram BM and Ramakrishna G (2014). Endoplasmic reticulum vacuolation and unfolded protein response leading to paraptosis like cell death in cyclosporine A treated cancer cervix cells is mediated by cyclophilin B inhibition. *Biochim Biophys Acta* **1843**, 2497–2512.
- [51] Walter P and Ron D (2011). The unfolded protein response: from stress pathway to homeostatic regulation. *Science* **334**, 1081–1086.
- [52] Sato A, Asano T, Ito K, Sumitomo M, and Asano T (2012). Suberoylanilide hydroxamic acid (SAHA) combined with bortezomib inhibits renal cancer growth by enhancing histone acetylation and protein ubiquitination synergistically. *BJU Int* **109**, 1258–1268.
- [53] Isono M, Sato A, Okubo K, Asano T, and Asano T (2016). Ritonavir interacts with belinostat to cause endoplasmic reticulum stress and histone acetylation in renal cancer cells. *Oncol Res* **24**, 327–335.
- [54] Isono M, Sato A, Asano T, Okubo K, and Asano T (2018). Delanzomib interacts with ritonavir synergistically to cause endoplasmic reticulum stress in renal cancer cells. *Anticancer Res* **38**, 3493–3500.
- [55] Okubo K, Sato A, Asano T, Isono M, and Asano T (2018). Nelfinavir induces endoplasmic reticulum stress and sensitizes renal cancer cells to TRAIL. *Anticancer Res* **38**, 4505–4514.
- [56] Sato A, Asano T, Ito K, and Asano T (2012). Vorinostat and bortezomib synergistically cause ubiquitinated protein accumulation in prostate cancer cells. *J Urol* **188**, 2410–2418.
- [57] Bali P, Pranpat M, Bradner J, Balasis M, Fiskus W, Guo F, Rocha K, Kumaraswamy S, Boyapalle S, and Atadja P, et al (2005). Inhibition of histone deacetylase 6 acetylates and disrupts the chaperone function of heat shock protein 90: a novel basis for antileukemia activity of histone deacetylase inhibitors. *J Biol Chem* **280**, 26729–26734.
- [58] Duo J, Ma Y, Wang G, Han X, and Zhang C (2013). Metformin synergistically enhances antitumor activity of histone deacetylase inhibitor trichostatin A against osteosarcoma cell line. *DNA Cell Biol* **32**, 156–164.
- [59] Chen H, Wang Y, Lin C, Lu C, Han R, Jiao L, Li L, and He Y (2017). Vorinostat and metformin sensitize EGFR-TKI resistant NSCLC cells via BIM-dependent apoptosis induction. *Oncotarget* **8**, 93825–93838.
- [60] Tang D, Xu L, Zhang M, Dorfman RG, Pan Y, Zhou Q, Wang Y, Li Y, Yin Y, and Wang L, et al (2018). Metformin facilitates BG45-induced apoptosis via an anti-Warburg effect in cholangiocarcinoma cells. *Oncol Rep* **39**, 1957–1965.